Research Article

Antioxidant Effects of Quercetin and Catechin Encapsulated into PLGA Nanoparticles

Hector Pool,[1] David Quintanar,[2] Juan de Dios Figueroa,[3] Camila Marinho Mano,[4] J. Etelvino H. Bechara,[4] Luis A. Godínez,[5] and Sandra Mendoza[1]

[1] *Departamento de Investigación y Posgrado en Alimentos, Facultad de Química, Universidad Autónoma de Queretaro, 76010 Queretaro, Mexico*
[2] *Laboratorio de Posgrado en Tecnología Farmacéutica, División de Estudios de Posgrado, Facultad de Estudios Superiores Cuautitlán, Universidad Nacional Autónoma de México, Cuautitlán Izcalli, 54740 Estado de México, Mexico*
[3] *Departamento de Materiales Bio-orgánicos, Centro de Investigación y Estudios Avanzados del Instituto Politécnico Nacional, Unidad Queretaro, 76230 Queretaro, Mexico*
[4] *Laboratorio de Radicais Livres e Estados Excitados em Sistemas Biologicos, Departamento de Bioquímica, Universidade de São Paulo, 05508-000 São Paulo, Brazil*
[5] *Centro de Investigación y Desarrollo Tecnológico en Electroquímica S.C., Pedro Escobedo, 76703 Querétaro, Mexico*

Correspondence should be addressed to Sandra Mendoza, smendoza@uaq.mx

Polymeric nanoparticles (PLGA) have been developed for the encapsulation and controlled release of quercetin and catechin. Nanoparticles were fabricated using a solvent displacement method. Physicochemical properties were measured by light scattering, scanning electron microscopy and ζ-potential, X-ray diffraction, infrared spectroscopy and differential scanning calorimetry. Encapsulation efficiency and *in vitro* release profiles were obtained from differential pulse voltammetry experiments. Antioxidant properties of free and encapsulated flavonoids were determined by TBARS, fluorescence spectroscopy and standard chelating activity methods. Relatively small ($d \approx 400$ nm) polymeric nanoparticles were obtained containing quercetin or catechin in a non-crystalline form (EE $\approx$ 79%) and the main interactions between the polymer and each flavonoid were found to consist of hydrogen bonds. *In vitro* release profiles were pH-dependant, the more acidic pH, the faster release of each flavonoid from the polymeric nanoparticles. The inhibition of the action of free radicals and chelating properties, were also enhanced when quercetin and catechin were encapsulated within PLGA nanoparticles. The information obtained from this study will facilitate the design and fabrication of polymeric nanoparticles as possible oral delivery systems for encapsulation, protection and controlled release of flavonoids aimed to prevent oxidative stress in human body or food products.

1. Introduction

Lipid oxidation is one of the most important processes that can cause deterioration in lipid bearing foods, which leads to the development of rancidity, off-flavor compounds, polymerization, and the decrease of the shelf life and nutritive value of food products [1, 2]. In addition, some studies have demonstrated that lipid oxidation is related to some stress oxidative diseases, such as diabetes mellitus, cancer, and cardiovascular diseases [3–6]. Oxidative degradation of lipids can be initiated by radical oxygen species (superoxide radicals, hydroxyl radicals, peroxyl radicals, etc.) and nonradical related compounds (hydrogen peroxide, singlet oxygen, ozone, etc.). Lipid oxidation can be accelerated by the presence of transition metal ions (Fe^{2+}, Cu^{1+}, Co^{1+}) which are present as ubiquitous impurities in food systems or human plasma [7, 8]. In this context, some methods have been used in order to delay the oxidation process in food products or in the human body. In this way, polyphenolic compounds, such as quercetin and catechin,

have gained great interest within the pharmaceutical and food industries due to their beneficial properties, such as antioxidant, antiradical, anti-inflammatory, antimutagenic, anticarcinogenic, antiangiogenic, antibacterial, antiviral, and antiaging effects, stimulating antioxidant enzymes in the human body [9–12]. Antiradical properties of quercetin and catechin have demonstrated that they can inhibit lipid oxidation in different systems; thus, catechin and quercetin have been proposed for the formulation of novel pharmaceutical or functional food products. However, the use of these two flavonoids has been limited due to their poor water solubility and instability under conditions encountered during food/pharmaceutical products processing (temperature, light, pH), in the gut (pH, enzymes, presence of other nutrients) or during storage (light, oxygen) [13, 14]. These factors limit the beneficial properties and potential health benefits of these compounds in functional food or pharmaceutical products [15]. Controlled delivery systems, such as nanoparticles, have shown their potential to protect, control the release, and increase the action of different bioactive compounds [16, 17].

Therefore, the aim of this study was to encapsulate quercetin or catechin within polymeric nanoparticles, using the biocompatible copolymer poly (D, L lactide-co-glycolide) (PLGA) and characterize their physicochemical and antioxidant properties. One of the most important aspects of this study is the determination of the encapsulation efficiency and *in vitro* release profiles at different pH values using differential pulse voltammetry (DPV). At the same time, evaluating the effect of free or encapsulated quercetin or catechin over free radicals that are produced during processes in the human body will facilitate the understanding of how these systems could act in novel commercial products or even in the human organism.

The knowledge obtained from this investigation could also facilitate the design of effective delivery systems for the encapsulation, protection, and release of bioactive flavonoids that have potential to improve human health or increase the shelf life of pharmaceutical or food products. These nanoparticulated systems may be suitable for their use in pharmaceutical applications and for the development of medical foods in the near future.

2. Materials and Methods

2.1. Materials. Quercetin, (+) catechin, polyvinyl alcohol (PVA), β-nicotinamide adenine dinucleotide (NADH), phenazine methosulfate (PMS), dimethylsulphoxide (DMSO), potassium bromide (KBr), and nitroblue tetrazolium (NBT) were purchased from Sigma Chemical Co. (St. Louis, MO, USA). 50 : 50 Poly (D, L-lactide-co-glycolide) (PLGA) was obtained from Lakeshore Biomaterials (Birmingham, AL, USA). Acetone and ethanol (analytical grade), phosphoric acid (H_3PO_4), boric acid (H_3BO_3), and acetic acid (CH_3–COOH) were obtained from J. T. Baker (Mallinckrodt Baker, Inc., Phillipsburg, NJ, USA). High quality water purified in a Milli-Q system (Millipore, Bedford, MD, USA) was used in all experiments.

2.2. Methods

2.2.1. Preparation of Polymeric Nanoparticles. PLGA nanoparticles were prepared by the solvent displacement method with minor modifications using a previously described protocol [18, 19]. PLGA (200 mg) was dissolved in 20 mL of acetone under magnetic stirring for 30 min at 25°C. The resulting PLGA solution was then slowly added to a 5% PVA aqueous solution (40 mL) using a syringe. The solution was then homogenized using a high shear mixer (Ultraturrax IKA T25, IKA/Works, Inc., NC, USA) at 19,000 RPM for 5 min. The organic solvent and water were evaporated for 30 min under vacuum using a rotary evaporator. The nanoparticles formed were washed with distilled water and ultracentrifuged (Optima XL-80K, Beckman Coulter, Inc., CA, USA) at 20,000 RPM for 20 min at 5°C. The pellet was resuspended in distilled water for 24 h and then stored for 12 h at −20°C in a freezer (General Electric, USA). The frozen nanoparticle dispersion was freeze dried at −70°C (10^{-3} Torr) for 48 h using a commercial freeze drier (LabconcoFreezone 6, Labconco Corp., MO, USA). The lyophilized nanoparticle dispersions were stored in desiccators containing dehydrating salts at 25°C until used. To prepare quercetin or catechin-loaded PLGA nanoparticles, separately, quercetin and catechin (10 mg) were dissolved into the PLGA-acetone solution prior to nanoparticle synthesis. Three independent batches of PLGA nanoparticles were prepared with or without quercetin or catechin for physicochemical and antioxidant characterizations.

2.2.2. Characterization

Particle Size and Charge Measurements. The mean particle diameter and polydispersity index (PI) of the nanoparticles were determined by dynamic light scattering (Nanosizer N4 Plus, Beckman Coulter Inc., CA, USA). The samples were diluted with distilled water to ensure that the number of particles counted per second was within the range of the instrument's sensitivity. Measurements were made at an angle of 90° for 180 s at 25°C. The electrical charge on the nanoparticles was measured by particle electrophoresis (Zetasizer Zen Systems 3600, Malvern Instruments Ltd., UK) after they had been diluted in deionized water to avoid multiple scattering effects and then placed in a folded capillary cell (25°C). Measurements were made in triplicate, and the results are shown as mean ± standard error.

Morphology. The morphology of the nanoparticles was studied by Environmental Scanning Electron Microscopy (ESEM). Nanoparticle samples were coated with a ≈20 nm gold film and then observed under high vacuum conditions within an electron microscope (Phillips XL30, FEI Company, OR, USA).

Determination of Drug Entrapment Efficiency (EE). Drug entrapment efficiency (EE) was determined by Differential Pulse Voltammetry (DPV) following a protocol previously described with minor modifications [20]. The electrochemical experiments were performed using a BAS-Epsilon

Potentiostat/Galvanostat instrument coupled to a C3-BAS Cell Stand. DPV experiments were performed in previously deoxygenated solutions by bubbling pure nitrogen gas for 20 min and using an electrochemical 10 mL cell in which a platinum (Pt) counter, a silver/silver chloride (Ag/AgCl), 3 M NaCl reference, and a glassy carbon working electrode (0.08 cm^2) were properly fitted. Before each experiment, the working electrode was polished using a slurry of 0.05 μm alumina particles dispersed in purified water on a felt surface. Parameters for DPV were 70 mV pulse amplitude and a scan rate of 5 mV/s. An aliquot of nanoparticles ($\approx$10 mg)

was dispersed in DMSO for 48 h by magnetic stirring in a glass vial covered with aluminum foil; pure nitrogen was bubbled before sealing the vial. 30 μL of nanoparticle/DMSO dispersions were then added to the electrochemical cell containing 3 mL of deoxygenated Britton-Robinson buffer pH 7. The flavonoid concentration was calculated used standard calibration curves. The flavonoid content remaining within the nanoparticles was calculated from the difference between the total amount of drug added and the amount of drug released in the aqueous medium. The encapsulation efficiency of the flavonoids was determined using as follows:

$$\text{EE (\%)} = \frac{\text{Amount of QC in entrapment} - \text{amount of QC in supernatant}}{\text{Total amount of QC in formulation}} \times 100. \tag{1}$$

2.2.3. Differential Scanning Calorimetry (DSC).
The phase behavior of quercetin, catechin, physical mixtures quercetin/PLGA, catechin/PLGA, quercetin-free, catechin-free, catechin-loaded, and quercetin-loaded nanoparticles (2.0 mg $\pm$ 0.2) was determined by DSC. The scan rate employed was 10°C/min in the temperature range from 0 to 340°C under nitrogen atmosphere at flow rate of 50 mL/min (DSC Q10, TA Instruments, DE, USA) [15]. Samples were analyzed in triplicate.

2.2.4. X-Ray Diffraction (XRD).
XRD patterns of quercetin, catechin, physical mixtures of quercetin/PLGA and catechin/PLGA, quercetin-free, catechin-free, and quercetin-loaded and catechin-loaded PLGA nanoparticles ($\approx$15 mg) were recorded using an X-ray diffraction instrument (Dmax 2100 Rigaku diffractometer, Rigaku Americas, TX, USA) employing a cobalt (Co) tube at λ = 1.78899 A, running at 30 kV and 16 mA.

2.2.5. Diffuse Reflectance of Infrared by Fourier Transform (DRIFT).
Infrared absorption spectra of quercetin, catechin, quercetin-free, catechin-free, and quercetin-loaded and catechin-loaded PLGA nanoparticles were examined by DRIFT spectroscopy (Spectrum GX spectrophotometer, Perkin-Elmer, MA, USA) with a diffuse reflectance accessory (Pike Technology model). All samples were previously stored in a desiccator containing silica gel at least 48 h at room temperature to ensure minimal moisture content. 2.4 mg of each sample were mixed with 97.6 mg of KBr, previously dried in an oven for 24 h at 135°C to remove moisture. The spectra were collected at 4 cm^{-1} resolution, with the wavenumber range of 400–4000 cm^{-1}. 16 scans were taken with the average from each spectrum recorded as ACII files. The pure KBr background spectrum was subtracted from the sample spectrum.

2.2.6. Drug In Vitro Release from Nanoparticles.
Drug *in vitro* release tests were performed using the described electrochemical protocol in [20]. Quercetin-loaded and catechin-loaded PLGA nanoparticles (5 mg) were added into

a Britton-Robinson buffer (pH adjusted to 7.4, 4.5, or 2 using HCl) and were magnetically stirred for 32 h. The amount of quercetin released from the nanoparticles was monitored at 0.25, 0.5, 1, 2, 4, 8, 12, 24, 26, 28, 30, and 32 h by the DPV technique. In order to maintain the chemical stability of quercetin released from nanoparticles during experiments, Britton-Robinson buffer was deoxygenated before each experiment, by bubbling high purity N$_2$ gas for 10 min in order to eliminate the presence of molecular oxygen that can oxidize the quercetin molecules.

2.2.7. Antioxidant Capacity of Free/Encapsulated Quercetin and Catechin

Superoxide Anion-Scavenging Activity Assay ($O_2^{\bullet -}$). The antioxidant capacity of free and encapsulated quercetin or catechin was estimated using the superoxide anion ($O_2^{\bullet -}$) scavenging activity assay, adapting our system to the previous established protocols [16]. $O_2^{\bullet -}$ radicals were formed in phosphate buffer (PBS) 0.1 M at pH 8. In a quartz cuvette PBS (1.2 mL), β-nicotinamide adenine dinucleotide (NADH, reduced form, 0.7 mM)/nitroblue tetrazolium (NBT, 17 mM) (800 μL), and 200 μL of Qc/Cate-loaded NPs solutions at three different flavonoid concentrations (7, 21 and 35 μM, adjusted to the NBT final concentration) were added. The mixture was kept in incubation for 120 min in a Varian Cary 50-Bio UV-Vis spectrophotometer (Agilent Technologies Brasil, SP, Brazil) under magnetic stirring (500 RPM) at 37°C. After incubation, 200 μL of phenazine methosulfate (PMS) (diluted in PBS pH 8, 4 μM) were added. The inhibition of NBT oxidation was continuously monitored for two minutes at 560 nm. PBS and PLGA/PBS solutions were used as negative controls and flavonoid standards were used as positive controls. The inhibition of NBT oxidation was calculated using as follows:

$$I(\%) = 100 - \frac{K_1}{K_0} \times 100, \tag{2}$$

where I is the percentage of oxidation inhibition, K_1 is the slope variation of the sample, and K_0 corresponds to

the slope variation of the blank. Samples were analyzed in triplicate (each batch) and the results are shown as mean ± SE.

Lipid Peroxidation Assay by Fluorescence. We evaluated the ability of free or encapsulated quercetin and catechin to inhibit the peroxidation of liposomes by peroxyl radicals, following established protocols [21]. Briefly, multilamellar vesicles of soybean phosphatidylcholine [22] at an initial concentration of 2.8 mM in phosphate buffer (PBS, 50 mM, pH 7.4) were prepared by vortexing and then by sonication for 14 min at 35°C. Unilamellar PC liposomes were obtained by extruding at least 15 times the multilamellar PC liposomes suspension through a Mini-Extruder (Avanti Polar Lipids, Inc., USA) within a 0.1 μm polycarbonate membrane. The resulting solution was kept at 5°C and protected from light until use. An oxidation-sensitive fluorescent dye 4,4-difluoro-5-(4-phenyl-1,3-butadienyl)-4-bora-3a,4a-diaza-s-indacene-3-undecanoic (C11-BODIPY$^{581/591}$) (40 μm) was incorporated into the bilayer structure of the phospholipid liposomes. Then, in a quartz cuvette 700 μL of PC/C11-BODIPY$^{581/591}$ solution, 250 μL of free/encapsulated quercetin solution at three different concentrations (0.02, 0.06, and 0.1 μM in PBS 50 mM, pH 7.4), and 50 μL of 2,2′-azobis (2′-methylpropionamidine) dihydrochloride (AAPH, 100 mM) to initiate the reduction of C11-BODIPY$^{581/591}$ were placed. Samples were magnetically stirred at 37°C for 2 min and then analyzed using a fluorescence spectrophotometer (F-4500, Hitachi, Ltd., USA). The fluorescence kinetics was continuously monitored for 60 min ($\lambda_{\text{excitation}}$ = 580 nm, 600 nm = $\lambda_{\text{emission}}$, Excitation slit = 10 nm, Emulsion slit = 5 nm). PBS 50 mM, pH 7.4 was used as negative control.

Metal Chelating Activity Assay. The chelating activity of Fe^{2+} was measured adapting our system to previously established protocols [23, 24]. Briefly, free or encapsulated quercetin and free or encapsulated catechin were kept separately under magnetic stirring at 42 rpm for 30 hrs at 25°C using a Daiki water bath equipped with magnetic stirring (Daiki Science Co., Ltd., Republic of Korea). Aliquots of each sample (500 μL) at 0, 4, 12, 18, 24 y 30 h were taken and ultracentrifuged at 12000 rpm for 5 min at 5°C using a Hermle refrigerated Z323K high performance centrifuge apparatus (HERMLE Labortechnik, Germany). Then 30 μL of the supernatant and 150 μL of FeCl$_2$ were added to a 96-well microplate. This mixture was allowed to stand for 5 min at darkness, and then 60 μL of ferrozine (5 mM) was added to the mixture, which was vigorously stirred and allowed to stand for 10 min in darkness. The absorbance of the solution was measured at 562 nm using a Spectra Max 190 microplate reader (Molecular Devices, Inc., USA). The percentage of iron chelating activity was calculated using as follows:

$$IC\ (\%) = 100 \times \left(1 - \frac{A_{\text{sample}}}{A_{\text{control}}}\right), \tag{3}$$

where A_{control} is the absorbance of Fe^{2+} + ferrozine and A_{sample} corresponds to the absorbance of a given sample.

Results were obtained from two individual experiments performance by triplicate. The results are expressed as mean ± SE.

3. Results

3.1. Physicochemical Properties of Nanoparticles

3.1.1. Morphological and Electrical Properties of Polymeric Nanoparticles. The functional performance of nanoparticle-based delivery systems depends on the physicochemical properties of the nanoparticles, such as size, morphology, charge, and physical state [25, 26]. We therefore measured the mean particle diameter and ζ-potential of the polymeric nanoparticles produced in this study (Table 1). Relatively small particles (mean diameters from 385 to 410 nm) with narrow distributions (PI from 0.173 to 0.39) were obtained. The electron microscopy images confirmed that the free and loaded PLGA nanoparticles were relatively small spheres with similar dimensions (Figure 2). These results disagree with other studies that have reported smaller ($\approx$200 nm) quercetin-loaded PLGA nanoparticles [27]. Molecular weight (MW), concentration of polymer used, and concentration of encapsulated active, are factors that can affect the final size of the particles [27, 28]. The MW of the PLGA used in this study was higher (60 kDa) than that used in other works; apparently the higher MW of the PLGA used in this study increased the viscosity of the internal phase, leading to a decreased net shear stress, thus producing larger nanoparticles. The PI values, on the other hand, indicated that the free and loaded nanoparticles obtained by the displacement solvent method were homogeneous, and that the method employed was reproducible and stable [29].

The electrical charge (ζ) of the free and loaded flavonoid polymeric nanoparticles was negative at pH 7, an observation that can be attributed to the presence of ionized carboxyl groups on the PLGA matrix [30]. Differences in ζ values were also observed between flavonoid free-nanoparticles and quercetin-loaded PLGA nanoparticles or catechin-loaded PLGA nanoparticles (-31.4 mV, -44.6 mV, and -29.8 mV, resp.). These results indicate that the presence of each specific flavonoid alter the electrical charge of the polymeric nanoparticles. However, the presence of each flavonoid within PLGA nanoparticles may not affect the stability of the nanoparticles given by ζ in aqueous dispersions. Some authors have indicated that with ζ values $\approx$+30 mV or $\approx$ -30 mV there are enough repulsion forces to avoid particle aggregation [31, 32]. Therefore, the ζ values for the polymeric nanoparticles obtained in this study indicate that there are strong electrostatic repulsion forces that prevent particle aggregation.

3.2. Encapsulation Properties of Polymeric Nanoparticles. The encapsulation efficiency (EE) of quercetin and catechin within the PLGA nanoparticles were around 79% and 76%, respectively, (Table 1). These results are lower than those of reported studies, where $\geq$95% of EE for quercetin in PLA nanoparticles were obtained [33]. Our results suggest that

TABLE 1: Mean particle size, polydispersity index, Zeta potential, and encapsulation efficiency of the PLGA NPs and quercetin/catechin-loaded PLGA NPs.

NPs		Particle size (nm)	Polydispersity index	Z potential (ζ) (mV)	E.E. (%)
PLGA	Placebo	387.27 ± 14.5[a]	0.173 ± 0.092[a]	−31.47 ± 1.01[a]	—
	Quercetin	399.67 ± 10.86[a]	0.262 ± 0.16[b]	−44.67 ± 0.48[b]	79.84 ± 2.5[a]
	Catechin	410.59 ± 9.66[a]	0.39 ± 0.125[c]	−29.83 ± 0.21[a]	76.14 ± 6.13[a]

Results are expressed as the mean ± S. E. of three replicates with three repetitions. Different letters indicate significant difference ($P < 0.05$) between rows compared with placebo PLGA.

(a)   (b)
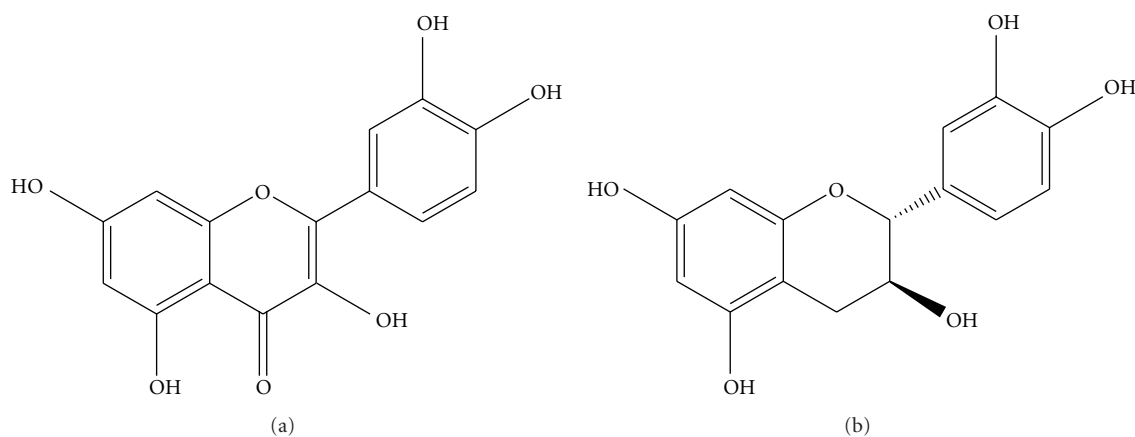
FIGURE 1: Molecular structure of quercetin (a) and catechin (b).

some quercetin may have been present within the surrounding aqueous phase, promoted apparently by the concentration of PVA used, which increased the water solubility of both flavonoids and thus more flavonoid molecules may partition out rapidly to the aqueous phase during the emulsification process therefore decreasing EE [27, 34].

3.3. Characterization of Nanoparticle Matrix Properties. Information on the structural organization of the bioactive molecules and polymeric matrix within the nanoparticles was determined by differential scanning calorimetry (DSC), infrared spectroscopy, and X-ray diffraction.

DSC is a powerful tool for the analysis of polymer-drug interactions and has previously been used to show that the drug and polymer are molecularly dispersed [35]. The phase transition analyses of quercetin, catechin, physical mixtures of quercetin/PLGA and catechin/PLGA, free-flavonoid PLGA nanoparticles, and flavonoid-loaded PLGA nanoparticles are shown in Figure 3. The DSC curves of quercetin (Figure 3(a)) showed two endothermic transitions at 134 and 325°C corresponding to dehydration (solid quercetin is initially hydrated) and melting of quercetin, respectively, [15, 36]. The DSC curves for catechin (Figure 3(b)) showed different endothermic transitions at 122 and 144°C, which correspond to the dehydration of hydrated catechin standard, 175 and 215°C related to the melting point of catechin conformers and at 294°C corresponding to the decomposition of the catechin molecule [37, 38]. For flavonoid-free PLGA nanoparticles, the DSC curves showed one endothermic peak around 52°C, corresponding to the glass transition

temperature (T_g) of the polymer [39, 40]. Physical mixtures of quercetin/PLGA and of catechin/PLGA (Figures 3(a) and 3(b), resp.) gave DSC profiles that exhibited a series of thermal transitions that correspond to those observed for PLGA, quercetin, and for catechin alone. However, there were some changes in the location of these transition peaks and some newly formed signals; these changes in peak positions suggest that there were interactions between PLGA and quercetin or catechin that resulted in the formation of a new structural organization of polymer and flavonoid, For quercetin-loaded or catechin-loaded PLGA nanoparticles, the DSC curves showed no thermal transitions corresponding to pure quercetin or pure catechin but showed a shifted endothermic peak that correspond to the T_g of the PLGA polymer. These results indicate that quercetin or catechin is dispersed in a noncrystalline state within the polymeric matrix of PLGA nanoparticles. Also, the shift in the T_g of the PLGA polymer suggests weak interactions between the PLGA matrix and quercetin or catechin, as described above. Our results are supported by the findings of other authors [29, 40–42].

The XRD patterns for both flavonoids, physical mixtures of each flavonoid with PLGA, free PLGA nanoparticles, and flavonoid-loaded PLGA nanoparticles are shown in Figure 4. For PLGA, the XRD pattern showed no peak, a fact that indicated that the polymer is amorphous [40, 42]. Pure quercetin and pure catechin exhibited characteristic signals of their crystalline structures [43–45]. The physical mixtures of quercetin and PLGA and catechin and PLGA also exhibited a number of different peaks; however, these peaks were
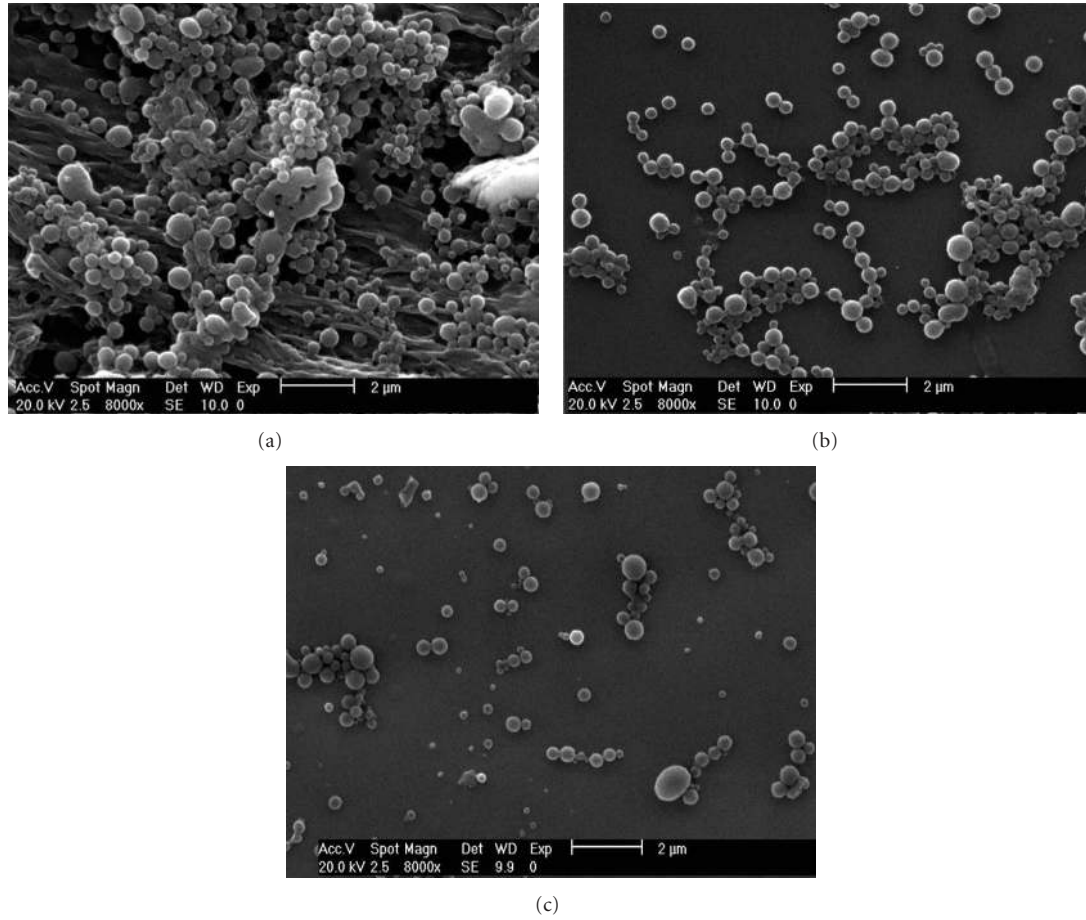
(a)

(b)

(c)

FIGURE 2: SEM micrographies of PLGA nanoparticles (a), quercetin-loaded PLGA nanoparticles (b), and catechin-loaded PLGA nanoparticles (c).

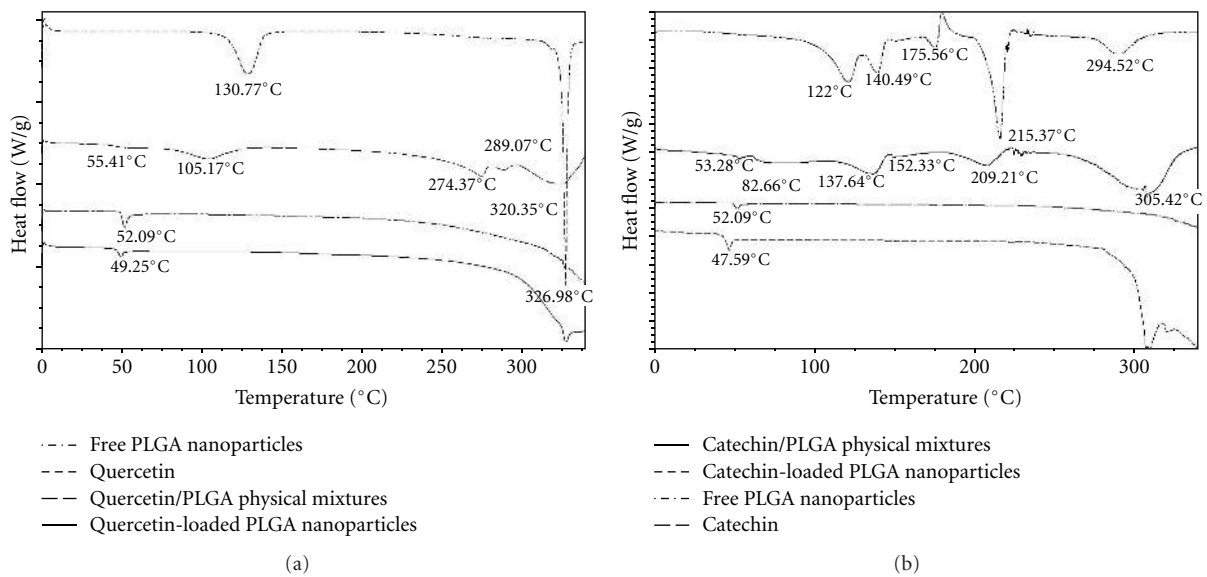Free PLGA nanoparticles
Quercetin
Quercetin/PLGA physical mixtures
Quercetin-loaded PLGA nanoparticles

(a)

Catechin/PLGA physical mixtures
Catechin-loaded PLGA nanoparticles
Free PLGA nanoparticles
Catechin

(b)
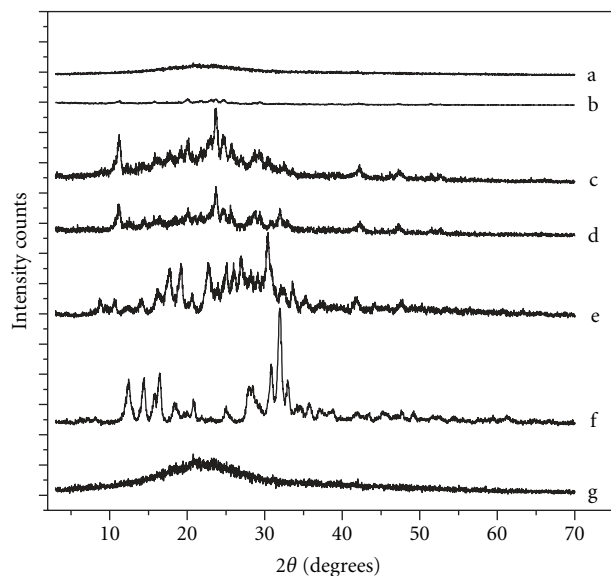
FIGURE 3: DSC thermograms for free PLGA nanoparticles (a) and (b), quercetin (a), quercetin/PLGA physical mixtures (a), and quercetin-loaded PLGA nanoparticles (a), catechin (b), catechin/PLGA physical mixtures (b), and catechin-loaded PLGA nanoparticles (b).

FIGURE 4: XRD spectra of catechin-loaded PLGA nanoparticles (a), quercetin-loaded PLGA nanoparticles (b), catechin/PLGA physical mixtures (c), quercetin/PLGA physical mixtures (d), catechin (e), quercetin (f), and free PLGA nanoparticles (g).
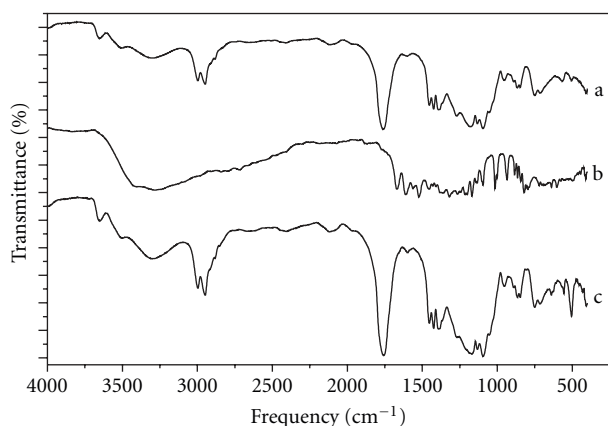
FIGURE 5: DRIFT spectra of free PLGA nanoparticles (a), quercetin (b), and quercetin-loaded PLGA nanoparticles (c). DRIFT spectrum is the mean of 16 scans.

slightly shifted from their original positions, and also while new peaks were observed, others disappeared. These results confirmed the findings obtained from DSC experiments and suggest that weak interactions occur between quercetin or catechin with the PLGA polymer matrix. The absence of peaks corresponding to the pure flavonoids on the XRD patterns for quercetin-loaded PLGA nanoparticles or catechin-loaded PLGA nanoparticles indicate that each flavonoid mainly exists dispersed in a noncrystalline state within the PLGA polymeric matrix.

Information on the nature of the molecular interactions within the solid matrix of the nanoparticles was obtained using Diffuse Reflectance of Infrared by Fourier Transform (DRIFT) [46]. DRIFT spectra for pure quercetin, pure
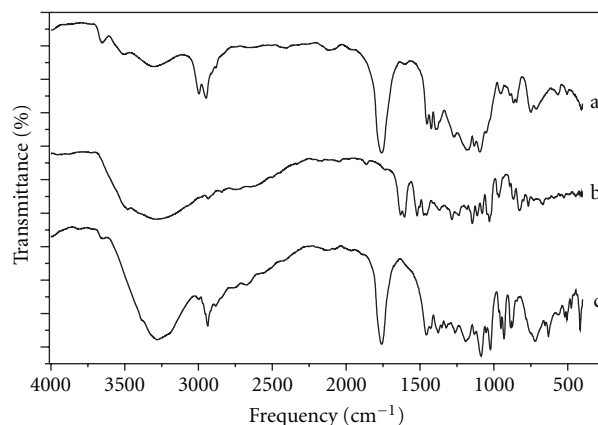

FIGURE 6: DRIFT spectra of free PLGA nanoparticles (a), catechin (b), and catechin-loaded PLGA nanoparticles (c). DRIFT spectrum is the mean of 16 scans.

catechin, active-free PLGA nanoparticles, quercetin-loaded PLGA nanoparticles, and catechin-loaded PLGA nanoparticles are shown in Figures 5 and 6. The DRIFT spectra for free PLGA nanoparticles showed the characteristic bands of the polymer, $-CH$, $-CH_2$, $-CH_3$ stretching (2850–3000 cm^{-1}), carbonyl $-C=O$ stretching (1700–1800 cm^{-1}), C–O stretching (1050–1250 cm^{-1}), and $-OH$ stretching (3200–3600 cm^{-1}) [34, 40]. For quercetin, the DRIFT spectra showed the characteristic bands corresponding to OH groups (3700–300 cm^{-1}), to C=O absorption (1662 cm^{-1}), bands of C–C stretching (1618 cm^{-1}), C–H bending (1456, 1383, and 866 cm^{-1}), a band attributed to the C–O stretching of the oxygen in the ring (1272 cm^{-1}), and the region for C–O stretching (1070–1150 cm^{-1}). These findings are consistent with previous studies [44, 46]. For pure catechin, DRIFT spectra exhibited the characteristic bands corresponding to OH stretching (3600–3200 cm^{-1}), C=C stretching (1600–1400 cm^{-1}), O–H stretching (1800–1670 cm^{-1}), C–O stretching of the oxygen in the ring (1272 cm^{-1}), and the characteristic peaks for the disubstituted aromatic ring (1200–900 cm^{-1}). The presence of these bands is also in agreement with previous studies [37, 47]. For quercetin-loaded and catechin-loaded PLGA nanoparticles, DRIFT showed that the OH stretching band (3200–3600 cm^{-1}) is slightly shifted and increased in terms of energy absorption. These observations suggest that quercetin and catechin are associated with the PLGA polymer by hydrogen bonds. Also, in the quercetin-loaded PLGA nanoparticles, the band corresponding for C=O stretching (1700–1800 cm^{-1}) was broader, indicating that quercetin is associated with the PLGA polymer by interactions between the carbonyl and the carboxyl groups of the flavonoid and the polymer. In addition, DRIFT measurements confirmed the encapsulation of quercetin and catechin within the PLGA nanoparticles.

3.4. Quercetin and Catechin Release from Nanoparticles. In this section, we investigated the release of quercetin and catechin from PLGA nanoparticles as a function of pH. The experiments were performed using a Briton-Robinson
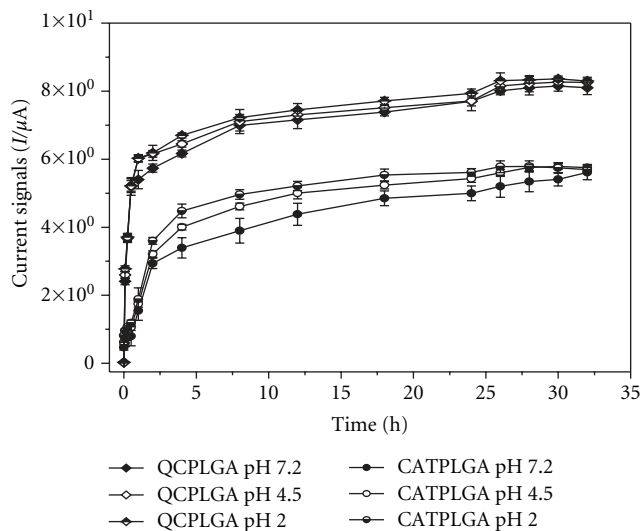
Figure 7: Current signals of quercetin and catechin obtained by the release from loaded PLGA nanoparticles at Britton-Robinson buffer (pH 2, 4.5, and 7.2) during 32 h of analysis period. Results are expressed as mean ± SD of three individual experiments.
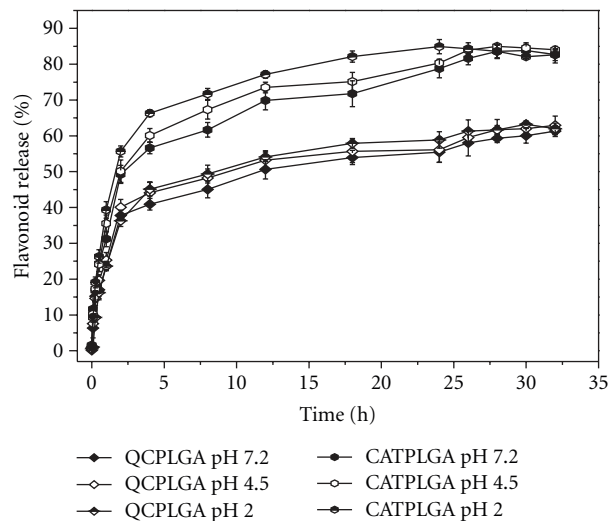

Figure 8: Percentage of quercetin and catechin released from PLGA nanoparticles in Britton-Robinson buffer (pH 2, 4.5, and 7.2). Results are expressed as mean ± SD of three individual experiments.

buffer at different pH values, simulating the pH conditions of the stomach (2–4.5) and from the small intestine (6-7), in the absence of enzymes. These results may be helpful for understanding the protection and release of bioactive flavonoids within acidic pH conditions, such as stomach or some food products, and at neutral pH conditions in the small intestine. In this way, we determined the *in vitro* release profiles for each flavonoid from polymeric nanoparticles using a different method from those that have been commonly used (e.g., HPLC, UV-VIS, and fluoresce spectroscopy). The advantage of using DPV is that this technique allows to monitor in real time the release of the bioactive compounds from the nanoparticles, using at the same time low amounts of solvents and thus lowering the experimentation costs.

Figure 7 shows the current responses ($I/\mu A$) obtained for quercetin and for catechin release from PLGA NPs in Britton-Robinson buffer (pH 7.2, 4.5, and 2) during a 32 h time period. These values were interpolated in calibration curves (concentration versus current responses) that were used to determine the concentration and percentage of flavonoid released during the experimentation time. The *in vitro* release of quercetin and catechin from PLGA nanoparticles (Figure 8) showed a biphasic release in the first 4 h, followed by a more gradual release at longer times until 65% and 85% of released quercetin and catechin, respectively, were achieved. As some authors have claimed, the burst release of each flavonoid species can be attributed to the diffusion of flavonoid molecules that are dispersed closer to the surface of the PLGA nanoparticles [28, 41, 48]. In addition, these profiles showed that as the pH becomes more acid, the release of both flavonoids is increased. This finding is related to the PLGA degradation, which is promoted in acidic media [49]. The differences observed in the release of quercetin

and catechin are related to specific interactions of the PLGA polymer and each flavonoid. The release of quercetin, for instance, is slower than that of catechin. This observation is probably due to an additional interaction of quercetin with PLGA, the interaction between carbonyl and carboxyl groups of the polymer and flavonoid molecules. As expected, some studies have demonstrated that when the polymer and the encapsulated active compounds have carboxyl-carbonyl interactions, the release rate of the active species decreases remarkably [30]. Therefore, catechin, which does not have a carboxyl group in its chemical structure (Figure 1), is released faster from PLGA nanoparticles than quercetin.

3.5. Antioxidant Capacity

3.5.1. Superoxide Anion-Scavenging Activity Assay ($O_2^\bullet$). We also evaluated the capacity of free or encapsulated quercetin and of free or encapsulated catechin to inhibit the action of the $O_2^\bullet$ radical. In the NBT/NADH system, PMS reacts with NADH removing an electron, which is transferred to molecular O_2, generating the radical $O_2^\bullet$. This radical species readily reduces NBT, causing the formation of a purple color and the consequent formation of formazan precipitates. Figure 9 shows the percentages of NBT reduction of free PLGA nanoparticles, free or encapsulated quercetin, and free or encapsulated catechin. Our results showed that encapsulated quercetin or catechin produced greater inhibition of NBT reduction than free flavonoids. These findings suggest that the flavonoid molecules dispersed in the PLGA nanoparticles are protected from molecular oxygen that could be produced during the 2 h stirring incubation process. Therefore, after incubation, encapsulated quercetin or catechin were released and scavenged the $O_2^\bullet$ radicals, as opposed to the case of free flavonoids, which are degraded after incubation, therefore decreasing their scavenger activity. Even when we showed that catechin is more rapidly released from PLGA
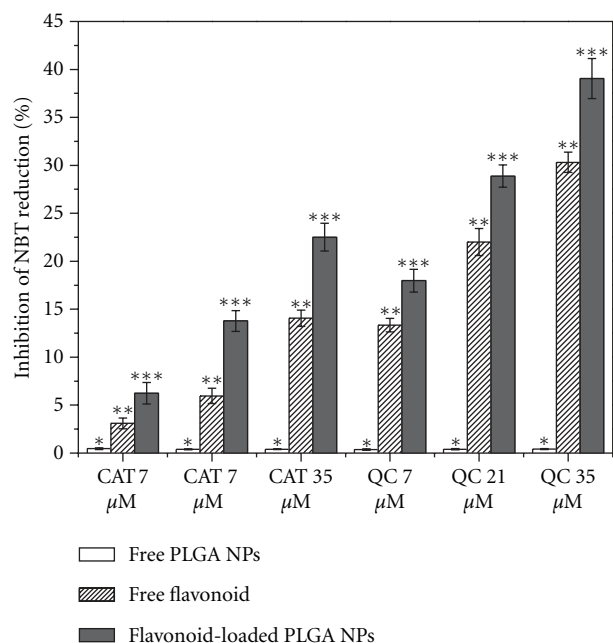
FIGURE 9: Inhibition of NBT reduction of free quercetin, free catechin, quercetin-loaded PLGA nanoparticles, and catechin-loaded PLGA nanoparticles at three different concentrations (7, 21, and 35 μM). All results are expressed as mean ± SE of three repetitions with at least two replicates. $**$ and $***$ significantly different ($P < 0.5$) from free flavonoids (positive control) and free PLGA NPs (negative control).

nanoparticles, quercetin showed a higher radical scavenging activity, mainly due to the presence of the C=O group and a double bond between C-2 and C-3 in the ring C in the quercetin structure, which allows this species to have a greater antiradical activity than catechin [50–52]. These results suggest that quercetin-loaded PLGA nanoparticles may be suitable to protect food from rancidity lead by free radical such as superoxide anion radicals.

3.5.2. Lipid Peroxidation Assay by Fluorescence. As previously mentioned, lipid oxidation is one of the most problematic deterioration processes occurring in foods containing unsaturated lipids, which leads to the development of rancidity, off-flavors, and polymerization reactions that reduce the shelf life and nutritive value of food products. Lipid oxidation may also generate undesirable biologically active species that are involved in cardiovascular and inflammatory disease processes [53–55]. For these reasons, we evaluated the ability of free and encapsulated flavonoids to inhibit lipid peroxidation of phospholipid liposomes. In this way, the ability of free and encapsulated quercetin and free and encapsulated catechin to inhibit lipid peroxidation was also monitored using fluorescent spectroscopy (Figure 10). An oxidation-sensitive fluorescent dye (C11-BODIPY$^{581/591}$) was incorporated into the bilayer structure of the phospholipid liposomes. This dye loses fluorescence when it is reduced by peroxyl (ROO$^\bullet$) radicals, and so a reduction in the fluorescence decay rate is evidence for protection against
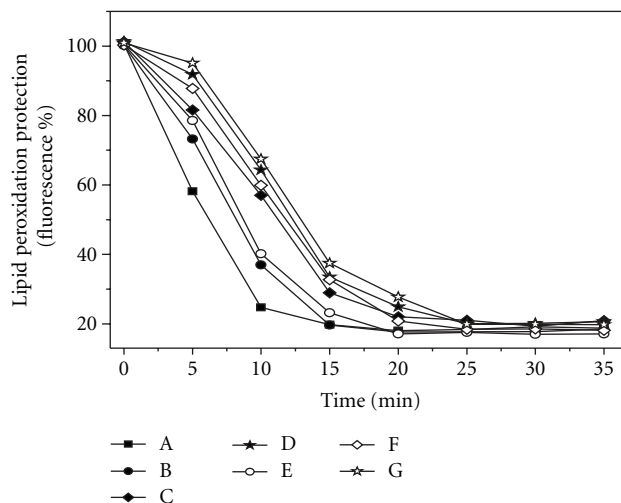

FIGURE 10: Lipid peroxidation protection by negative control (PBS, A), free quercetin 1 μM (B), free quercetin 3 μM (C), free quercetin 5 μM (D), encapsulated quercetin 1 μM (E), encapsulated quercetin 3 μM (F), and encapsulated quercetin 5 μM (G). Values represent the means of three individual measurements.
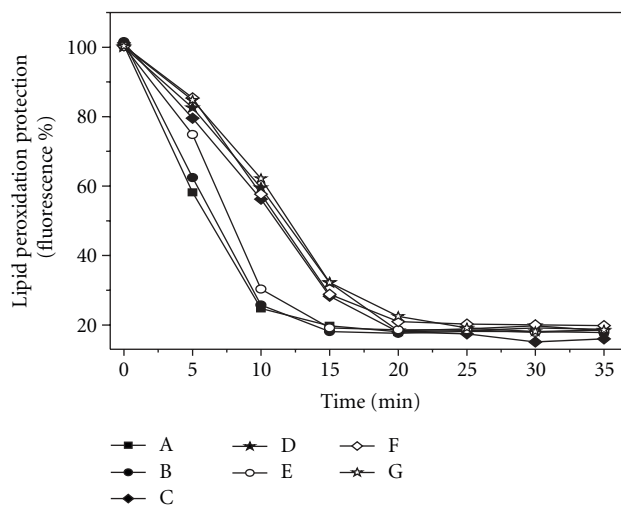

FIGURE 11: Lipid peroxidation protection by negative control (PBS, A), free catechin 1 μM (B), free catechin 3 μM (C), free catechin 5 μM (D), encapsulated catechin 1 μM (E), encapsulated catechin 3 μM (F), and encapsulated catechin 5 μM (G). Values represent the means of three individual measurements.

lipid oxidation. Free or encapsulated quercetin was added to the solution containing phospholipid liposomes 2 hours before starting the reduction reaction. A reducing agent (AAPH) was then added to the system to promote lipid peroxidation. Figures 10 and 11 show the fluorescence decay rates of C11-BODIPY$^{581/591}$ by ROO$^\bullet$ radicals and the effect of free and encapsulated quercetin and catechin. As expected, the evaluated systems inhibit the peroxidation reaction in a concentration dependent manner. The lipid oxidation inhibition was greater when quercetin or catechin were dispersed within PLGA nanoparticles than when dispersed in water.
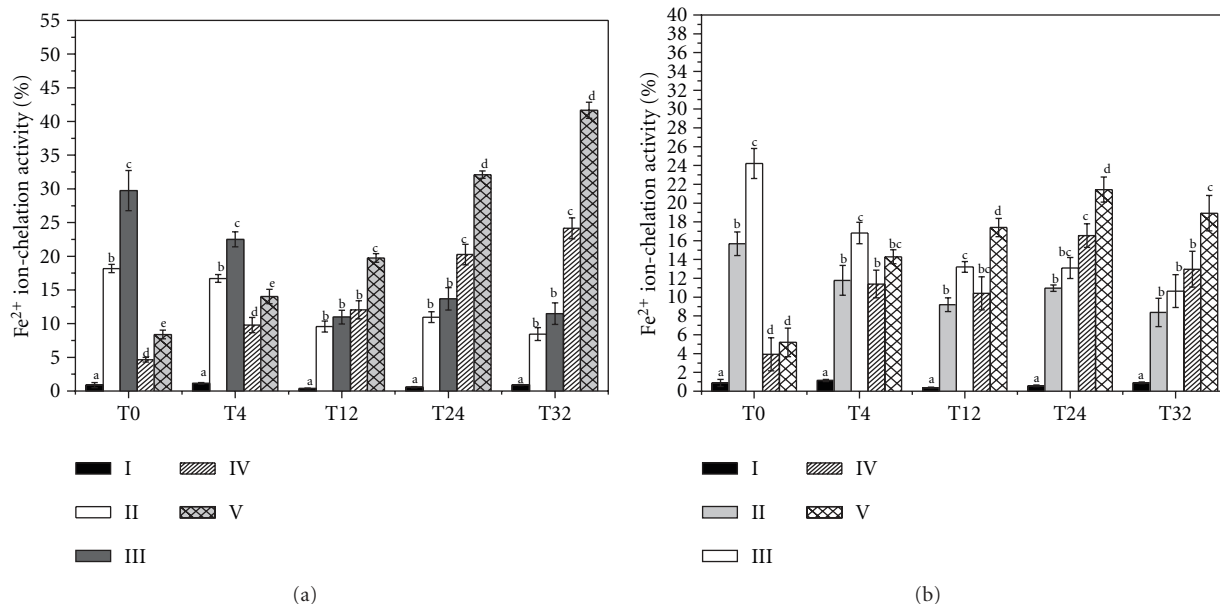
(a)

(b)

FIGURE 12: Chelating activity of Fe^{2+} ions by free PLGA nanoparticles (aI, bI), free quercetin $20\,\mu M$ (aII), free quercetin $100\,\mu M$ (aIII), encapsulated quercetin $20\,\mu M$ (aIV), encapsulated quercetin $100\,\mu M$ (aV), free catechin $20\,\mu M$ (bII), free catechin $100\,\mu M$ (bIII), encapsulated catechin $20\,\mu M$ (bIV), and encapsulated catechin $10\,\mu M$ (bV). Different letters represent significantly difference ($P < 0.05$) between treatments at one specific time of experimentation (0.25, 4, 12, 24, and 32 h). Results are represented by the mean ± SE.

These results can be attributed to the protection of PLGA nanoparticles during the incubation process to which they were submitted during 2 h. Molecular oxygen formed by the stirring process could degrade the unprotected flavonoids, thus decreasing their antiradical properties. These results showed that the antiradical capacity of both encapsulated flavonoids remains after the encapsulation process. These findings too suggest that these polymeric nanoparticles may be useful for the incorporation of bioactive flavonoids with the aim of inhibiting lipid oxidation reactions in either food products or the human body.

3.5.3. Chelating Activity of Flavonoid-Loaded PLGA NPs. Chelating activity directly influences the generation of oxidant species thus constituting an important factor of the antioxidant properties of a compound or system [24]. Thus, the ability to chelate iron ions (Fe^{2+}) by free and encapsulated flavonoids was evaluated (Figure 12). It can be observed that the chelating activity of free quercetin and free catechin (Figures 12(a) and 12(b), resp.) decreased over time (0–32 hrs). This might be due to the degradation of flavonoid molecules by molecular O_2 formed during the incubation and stirring processes. Encapsulated quercetin and encapsulated catechin demonstrated an increase in the chelating properties of Fe^{2+} ions. Protection of PLGA nanoparticles allowed encapsulated quercetin or catechin to remain stable during the time of experimentation, leading to exerting their chelating capacity. In addition, it has been suggested that the ultracentrifugation method might affect the release of encapsulated actives, forcing a faster diffusion and spreading the molecules that are closer to the nanoparticle surface and thus may produce a major

release of flavonoids from nanoparticles that reacted with iron ions. Moreover, drug release from PLGA nanoparticles could be increased by degradation of PLGA chains in the presence of water by hydrolysis [30]. Although catechin has a faster release from the polymeric nanoparticles compared to quercetin, the chelating capacity of encapsulated quercetin was higher, mainly due to its higher capacity to chelate transition metal ions, as has been reported by other authors [23, 56, 57].

4. Conclusions

Polymeric nanoparticles were prepared and used to encapsulate, protect, and release two bioactive flavonoid molecules, quercetin and catechin. We showed that both flavonoids were successfully encapsulated in a noncrystalline state within the PLGA nanoparticles matrix, with an EE of ≈79%. Also we showed that the release profile method used is suitable, reproducible, and stable for these types of determinations. The *in vitro* release profiles showed that quercetin and catechin release rates are pH-dependent, liberating them in a higher rate when the pH conditions of the environment are more acidic. These results suggest that PLGA nanoparticles could be suitable for the encapsulation of bioactive compounds (such as flavonoids and vitamins) and to release them in acidic environments, such as the stomach of some food products. These findings could also be useful for the design and fabrication of polymeric nanoparticles for the targeted release of these compounds within stomach for the treatment of local diseases or to release them in acidic food products, producing novel functional foods. Also this study showed that the use of PLGA nanoparticles increase the

antiradical and chelating properties of these two flavonoids. Therefore, these delivery systems may be suitable to increase the shelf life of lipid food products or may be helpful as novel therapeutic systems to delay the development of diseases related to oxidative stress (e.g., diabetes mellitus and cancer). Nevertheless, more studies are necessary to demonstrate that PLGA nanoparticles can protect and release these bioactive flavonoids within the gastrointestinal tract, evaluating their bioaccessibility and bioavailability. Also studies of the incorporation, release, and protection on a model food product may be important to investigate. In general, our results have important implications for the design and fabrication of polymeric nanoparticle delivery systems for bioactive compounds with beneficial properties for human health and wellness.
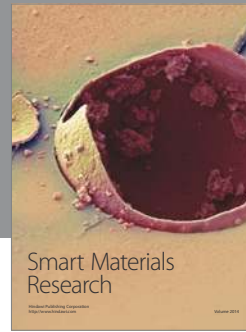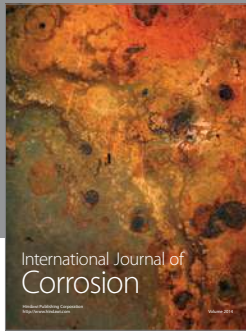
Acknowledgments

References

[1] C. C. Akoh and D. B. Min, *Food Lipids: Chemistry, Nutrition, and Biotechnology*, CRC, 2008.

[2] D. B. Min and J. M. Boff, "Lipid oxidation of edible oil," in *Food Lipids: Chemistry, Nutrition, and Biotechnology*, pp. 335–364, Marcel Dekker, New York, NY, USA, 2002.

[3] S. Seki, T. Kitada, T. Yamada, H. Sakaguchi, K. Nakatani, and K. Wakasa, "In situ detection of lipid peroxidation and oxidative DNA damage in non-alcoholic fatty liver diseases," *Journal of Hepatology*, vol. 37, no. 1, pp. 56–62, 2002.

[4] J. W. Baynes and S. R. Thorpe, "Role of oxidative stress in diabetic complications: a new perspective on an old paradigm," *Diabetes*, vol. 48, no. 1, pp. 1–9, 1999.

[5] H. Bartsch and J. Nair, "Oxidative stress and lipid peroxidation-derived DNA-lesions in inflammation driven carcinogenesis," *Cancer Detection and Prevention*, vol. 28, no. 6, pp. 385–391, 2004.

[6] M. D. Gross, "Lipids, oxidation, and cardiovascular disease," in *Atherosclerosis and Oxidant Stress*, pp. 79–95, Springer, 2008.

[7] J. Vercellotti, A. J. S. Angelo, and A. M. Spanier, "Lipid oxidation in foods," in *Lipid Oxidation in Food*, vol. 500, pp. 1–11, American Chemical Society, 1992.

[8] B. Halliwell, S. Chirico, M. A. Crawford, K. S. Bjerve, and K. F. Gey, "Lipid peroxidation: its mechanism, measurement, and significance," *American Journal of Clinical Nutrition*, vol. 57, no. 5, pp. 715S–724S, 1993.

[9] G. Galati and P. J. O'Brien, "Potential toxicity of flavonoids and other dietary phenolics: significance for their chemopreventive and anticancer properties," *Free Radical Biology and Medicine*, vol. 37, no. 3, pp. 287–303, 2004.

[10] I. Erlund, "Review of the flavonoids quercetin, hesperetin, and naringenin. Dietary sources, bioactivities, bioavailability, and epidemiology," *Nutrition Research*, vol. 24, no. 10, pp. 851–874, 2004.

[11] L. H. Yao, Y. M. Jiang, J. Shi et al., "Flavonoids in food and their health benefits," *Plant Foods for Human Nutrition*, vol. 59, no. 3, pp. 113–122, 2004.

[12] M. Friedman, "Overview of antibacterial, antitoxin, antiviral, and antifungal activities of tea flavonoids and teas," *Molecular Nutrition and Food Research*, vol. 51, no. 1, pp. 116–134, 2007.

[13] P. Ader, A. Wessmann, and S. Wolffram, "Bioavailability and metabolism of the flavonol quercetin in the pig," *Free Radical Biology and Medicine*, vol. 28, no. 7, pp. 1056–1067, 2000.

[14] L. Bell, "Stability testing of nutraceuticals and functional foods," in *Handbook of Nutraceuticals and Functional Foods*, pp. 501–516, CRC Press, 2001.

[15] G. S. Borghetti, I. S. Lula, R. D. Sinisterra, and V. L. Bassani, "Quercetin/β-Cyclodextrin solid complexes prepared in aqueous solution followed by spray-drying or by physical mixture," *AAPS PharmSciTech*, vol. 10, no. 1, pp. 235–242, 2009.

[16] A. Barras, A. Mezzetti, A. Richard et al., "Formulation and characterization of polyphenol-loaded lipid nanocapsules," *International Journal of Pharmaceutics*, vol. 379, no. 2, pp. 270–277, 2009.

[17] J. Weiss, E. A. Decker, D. J. McClements, K. Kristbergsson, T. Helgason, and T. Awad, "Solid lipid nanoparticles as delivery systems for bioactive food components," *Food Biophysics*, vol. 3, no. 2, pp. 146–154, 2008.

[18] R. Alvarez-Román, G. Barré, R. H. Guya, and H. Fessi, "Biodegradable polymer nanocapsules containing a sunscreen agent: preparation and photoprotection," *European Journal of Pharmaceutics and Biopharmaceutics*, vol. 52, no. 2, pp. 191–195, 2001.

[19] H. Fessi, F. Piusieux, J. P. Devissaguet, N. Ammoury, and S. Benita, "Nanocapsule formation by interfacial polymer deposition following solvent displacement," *International Journal of Pharmaceutics*, vol. 55, no. 1, pp. R1–R4, 1989.

[20] L. Mora, K. Y. Chumbimuni-Torres, C. Clawson, L. Hernandez, L. Zhang, and J. Wang, "Real-time electrochemical monitoring of drug release from therapeutic nanoparticles," *Journal of Controlled Release*, vol. 140, no. 1, pp. 69–73, 2009.

[21] R. C. MacDonald, R. I. MacDonald, B. P. M. Menco, K. Takeshita, N. K. Subbarao, and L. R. Hu, "Small-volume extrusion apparatus for preparation of large, unilamellar vesicles," *Biochimica et Biophysica Acta*, vol. 1061, no. 2, pp. 297–303, 1991.

[22] H. A. Morais, L. M. De Marco, M. C. Oliveira, and M. P. C. Silvestre, "Casein hydrolysates using papain: peptide profile and encapsulation in liposomes," *Acta Alimentaria*, vol. 34, no. 1, pp. 59–69, 2005.

[23] I. B. Afanas'ev, A. I. Dorozhko, A. V. Brodskii, V. A. Kostyuk, and A. I. Potapovitch, "Chelating and free radical scavenging mechanisms of inhibitory action of rutin and quercetin in lipid peroxidation," *Biochemical Pharmacology*, vol. 38, no. 11, pp. 1763–1769, 1989.

[24] M. A. Ebrahimzadeh, S. M. Nabavi, and S. F. Nabavi, "Correlation between the in vitro iron chelating activity and poly phenol and flavonoid contents of some medicinal plants," *Pakistan Journal of Biological Sciences*, vol. 12, no. 12, pp. 934–938, 2009.

[25] F. Ahsan, I. P. Rivas, M. A. Khan, and A. I. Torres Suárez, "Targeting to macrophages: role of physicochemical properties of particulate carriers—liposomes and microspheres—on the phagocytosis by macrophages," *Journal of Controlled Release*, vol. 79, no. 1-3, pp. 29–40, 2002.

[26] S. Galindo-Rodriguez, E. Allémann, H. Fessi, and E. Doelker, "Physicochemical parameters associated with nanoparticle formation in the salting-out, emulsification-diffusion, and nanoprecipitation methods," *Pharmaceutical Research*, vol. 21, no. 8, pp. 1428–1439, 2004.

[27] X. Song, Y. Zhao, S. Hou et al., "Dual agents loaded PLGA nanoparticles: systematic study of particle size and drug entrapment efficiency," *European Journal of Pharmaceutics and Biopharmaceutics*, vol. 69, no. 2, pp. 445–453, 2008.

[28] X. Song, Y. Zhao, W. Wu et al., "PLGA nanoparticles simultaneously loaded with vincristine sulfate and verapamil hydrochloride: systematic study of particle size and drug entrapment efficiency," *International Journal of Pharmaceutics*, vol. 350, no. 1-2, pp. 320–329, 2008.

[29] O. I. Corrigan and X. Li, "Quantifying drug release from PLGA nanoparticulates," *European Journal of Pharmaceutical Sciences*, vol. 37, no. 3-4, pp. 477–485, 2009.

[30] C. E. Astete and C. M. Sabliov, "Synthesis and characterization of PLGA nanoparticles," *Journal of Biomaterials Science, Polymer Edition*, vol. 17, no. 3, pp. 247–289, 2006.

[31] L. Qi, Z. Xu, X. Jiang, C. Hu, and X. Zou, "Preparation and antibacterial activity of chitosan nanoparticles," *Carbohydrate Research*, vol. 339, no. 16, pp. 2693–2700, 2004.

[32] J. Hu, K. P. Johnston, and R. O. Williams, "Nanoparticle engineering processes for enhancing the dissolution rates of poorly water soluble drugs," *Drug Development and Industrial Pharmacy*, vol. 30, no. 3, pp. 233–245, 2004.

[33] A. Kumari, S. K. Yadav, Y. B. Pakade, B. Singh, and S. C. Yadav, "Development of biodegradable nanoparticles for delivery of quercetin," *Colloids and Surfaces B*, vol. 80, no. 2, pp. 184–192, 2010.

[34] R. M. Mainardes and R. C. Evangelista, "PLGA nanoparticles containing praziquantel: effect of formulation variables on size distribution," *International Journal of Pharmaceutics*, vol. 290, no. 1-2, pp. 137–144, 2005.

[35] H. Eerikäinen and E. I. Kauppinen, "Preparation of polymeric nanoparticles containing corticosteroid by a novel aerosol flow reactor method," *International Journal of Pharmaceutics*, vol. 263, no. 1-2, pp. 69–83, 2003.

[36] S. Olejniczak and M. J. Potrzebowski, "Solid state NMR studies and density functional theory (DFT) calculations of conformers of quercetin," *Organic and Biomolecular Chemistry*, vol. 2, no. 16, pp. 2315–2322, 2004.

[37] K. Dias, S. Nikolaou, and W. F. De Giovani, "Synthesis and spectral investigation of Al(III) catechin/β-cyclodextrin and Al(III) quercetin/β-cyclodextrin inclusion compounds," *Spectrochimica Acta A*, vol. 70, no. 1, pp. 154–161, 2008.

[38] A. R. Dudhani and S. L. Kosaraju, "Bioadhesive chitosan nanoparticles: preparation and characterization," *Carbohydrate Polymers*, vol. 81, no. 2, pp. 243–251, 2010.

[39] M. Holzer, V. Vogel, W. Mäntele, D. Schwartz, W. Haase, and K. Langer, "Physico-chemical characterisation of PLGA nanoparticles after freeze-drying and storage," *European Journal of Pharmaceutics and Biopharmaceutics*, vol. 72, no. 2, pp. 428–437, 2009.

[40] R. M. Mainardes, M. P. D. Gremião, and R. C. Evangelista, "Thermoanalytical study of praziquantel-loaded PLGA nanoparticles," *Brazilian Journal of Pharmaceutical Sciences*, vol. 42, no. 4, pp. 523–530, 2006.

[41] M. D. Blanco and M. J. Alonso, "Development and characterization of protein-loaded poly(lactide-co-glycolide) nanospheres," *European Journal of Pharmaceutics and Biopharmaceutics*, vol. 43, no. 3, pp. 287–294, 1997.

[42] S. A. Joshi, S. S. Chavhan, and K. K. Sawant, "Rivastigmine-loaded PLGA and PBCA nanoparticles: preparation, optimization, characterization, in vitro and pharmacodynamic studies," *European Journal of Pharmaceutics and Biopharmaceutics*, vol. 76, no. 2, pp. 189–199, 2010.

[43] Y. Zhang, Y. Yang, K. Tang, X. Hu, and G. Zou, "Physicochemical characterization and antioxidant activity of quercetin-loaded chitosan nanoparticles," *Journal of Applied Polymer Science*, vol. 107, no. 2, pp. 891–897, 2008.

[44] T. H. Wu, F. L. Yen, L. T. Lin, T. R. Tsai, C. C. Lin, and T. M. Cham, "Preparation, physicochemical characterization, and antioxidant effects of quercetin nanoparticles," *International Journal of Pharmaceutics*, vol. 346, no. 1-2, pp. 160–168, 2008.

[45] Y. M. Chen, M. K. Wang, and P. M. Huang, "Catechin transformation as influenced by aluminum," *Journal of Agricultural and Food Chemistry*, vol. 54, no. 1, pp. 212–218, 2006.

[46] M. L. Calabrò, S. Tommasini, P. Donato et al., "Effects of α- and β-cyclodextrin complexation on the physicochemical properties and antioxidant activity of some 3-hydroxyflavones," *Journal of Pharmaceutical and Biomedical Analysis*, vol. 35, no. 2, pp. 365–377, 2004.

[47] M. M. Ramos-Tejada, J. D. G. Durán, A. Ontiveros-Ortega, M. Espinosa-Jimenez, R. Perea-Carpio, and E. Chibowski, "Investigation of alumina/(+)-catechin system properties. Part I: a study of the system by FTIR-UV-Vis spectroscopy," *Colloids and Surfaces B*, vol. 24, no. 3-4, pp. 297–308, 2002.

[48] C. Gómez-Gaete, N. Tsapis, M. Besnard, A. Bochot, and E. Fattal, "Encapsulation of dexamethasone into biodegradable polymeric nanoparticles," *International Journal of Pharmaceutics*, vol. 331, no. 2, pp. 153–159, 2007.

[49] J. Y. Yoo, J. M. Kim, K. S. Seo, Y. K. Jeong, H. B. Lee, and G. Khang, "Characterization of degradation behavior for PLGA in various pH condition by simple liquid chromatography method," *Bio-Medical Materials and Engineering*, vol. 15, no. 4, pp. 279–288, 2005.

[50] B. Havsteen, "Flavonoids, a class of natural products of high pharmacological potency," *Biochemical Pharmacology*, vol. 32, no. 7, pp. 1141–1148, 1983.

[51] M. A. Anagnostopoulou, P. Kefalas, V. P. Papageorgiou, A. N. Assimopoulou, and D. Boskou, "Radical scavenging activity of various extracts and fractions of sweet orange peel (*Citrus sinensis*)," *Food Chemistry*, vol. 94, no. 1, pp. 19–25, 2006.

[52] W. Bors, W. Heller, C. Michel, and M. Saran, "Flavonoids as antioxidants: determination of radical-scavenging efficiencies," *Methods in Enzymology*, vol. 186, pp. 343–355, 1990.

[53] W. Chaiyasit, R. J. Elias, D. J. McClements, and E. A. Decker, "Role of physical structures in bulk oils on lipid oxidation," *Critical Reviews in Food Science and Nutrition*, vol. 47, no. 3, pp. 299–317, 2007.

[54] B. Halliwell, M. A. Murcia, S. Chirico, and O. I. Aruoma, "Free radicals and antioxidants in food and in vivo: what they do and how they work," *Critical Reviews in Food Science and Nutrition*, vol. 35, no. 1-2, pp. 7–20, 1995.

[55] T. M. McIntyre and S. L. Hazen, "Lipid oxidation and cardiovascular disease: introduction to a review series," *Circulation Research*, vol. 107, no. 10, pp. 1167–1169, 2010.

[56] K. E. Heim, A. R. Tagliaferro, and D. J. Bobilya, "Flavonoid antioxidants: chemistry, metabolism and structure-activity relationships," *Journal of Nutritional Biochemistry*, vol. 13, no. 10, pp. 572–584, 2002.

[57] S. A. B. E. Van Acker, D. J. Van Den Berg, M. N. J. L. Tromp et al., "Structural aspects of antioxidant activity of flavonoids," *Free Radical Biology and Medicine*, vol. 20, no. 3, pp. 331–342, 1996.